Macroporous Vanadium Phosphorus Oxide Phases Displaying Three-Dimensional Arrays of Spherical Voids

Moises A. Carreon and Vadim V. Guliants*

Department of Chemical Engineering, University of Cincinnati, Cincinnati, Ohio 45221-0171

Received December 27, 2001. Revised Manuscript Received March 28, 2002

Macroporous vanadium phosphorus oxide (VPO) phases with remarkable compositional, structural, and morphological properties have been synthesized employing monodisperse polystyrene sphere arrays as a template. Colloidal polystyrene spheres were ordered into close-packed arrays by sedimentation or centrifugation. Depending on the choice of VPO sources and the template removal method, various crystalline VPO phases were obtained. The macroscale-templated synthesis produced VPO phases with unprecedented high surface areas (75 m^2/g); desirable macroporous architecture; optimal bulk compositions (P/V $\approx$ 1.1); desirable vanadium oxidation states (4.1−4.4); and preferential exposure of the surface (100) planes of $VO_2P_2O_7$, the proposed active and selective phase for the partial oxidation of *n*-butane.

Introduction

Vanadium-containing mixed metal oxides exhibit highly promising catalytic properties for selective oxidation of lower alkanes.[1] For example, molybdenum vanadium niobium and antimony vanadium oxides are catalytically active in the oxidative dehydrogenation and selective oxidation of ethane[2] and the ammoxidation of propane.[3] Vanadium phosphorus oxide (VPO) is the only commercial catalytic system for the gas-phase selective oxidation of an alkane, i.e., *n*-butane to maleic anhydride.[4] Conventional synthesis methods for mixed metal oxides, both wet chemistry and solid-state, offer very limited control over desirable structural and compositional properties, such as the phase, bulk and surface compositions, preferential exposure of active and selective surface planes, surface areas, and pore architectures, which define their catalytic properties in the selective oxidation of lower alkanes.

The macroscale-templated synthesis of nanocrystalline mixed metal oxides is an attractive approach for the hierarchical design of catalytic materials that exhibit remarkable ordering on the micro- (<3 nm for the surface region structure and composition), nano- (3−100 nm for the bulk and phase compositions), and macro- (>100 nm for pore architectures) scales. In particular, templating against opaline arrays of colloidal spheres offers a general route to macroporous materials displaying controlled pore sizes, high surface areas, and highly ordered three-dimensional porous structures, which are very attractive for catalytic applications. Several single-element macroporous oxides with very interesting structural properties have been synthesized using colloidal sphere templates. Stein et al.[5−9] reported the synthesis of highly ordered macroporous TiO_2, ZrO_2, Al_2O_3, SiO_2, Fe_2O_3, Sb_4O_6 ,WO_3, MgO, Cr_2O_3, Mn_2O_3, NiO, ZnO, $CaCO_3$, and Co_3O_4 using ordered arrays of latex spheres as templates. Pine et al.[10,11] described the synthesis of ordered macroporous ZrO_2, TiO_2, and SiO_2 using an emulsion templating approach. Velev et al.[12−14] reported the synthesis of macroporous silica via colloidal crystallization. Vos et al.[15,16] described the synthesis of ordered macroporous TiO_2 and SiO_2 using a liquid-phase chemical reaction. However, only a few examples of macroporous binary oxides have been reported.[7,17] Stein et al.[7] prepared macroporous aluminophosphate by permeating an aluminum isopropoxide−phosphoric acid solution into a latex sphere array. Similarly, macroporous yttria−zirconia was prepared using alkoxides as metal sources. Macroporous silica−titania with tailored pore morphologies was synthesized via a colloidal templating method.[17] Recently, we reported the first successful example of a hierarchically structured macroporous *mixed* vanadium phosphorus oxide (macro-VPO) with desirable structural and compositional properties for the selective oxidation of *n*-butane.[18] We present here the

* To whom correspondence should be addressed. Phone: 513-556-0203. Fax: 513-556-3473. E-mail: Vadim.Guliants@UC.EDU.

(1) Trifiro, F. *Catal. Today* **1998**, *21*, 41.
(2) Bettahar, M. M.; Constentin, G.; Savary, L.; Lavalley, J. C. *Appl. Catal.* **1996**, *145*, 1
(3) Lin, M. M. *Appl. Catal.* **2001**, *207*, 1
(4) Centi , G. *Catal. Today* **1993**, *5*, 16.
(5) Holland, B. T.; Blanford, C. F.; Stein, A. *Science* **1998**, *281*, 538.
(6) Holland, B. T.; Abrams, L.; Stein, A. *J. Am. Chem. Soc.* **1999**, *121*, 4308.
(7) Holland, B. T.; Blanford, C. F.; Do, T.; Stein, A. *Chem. Mater.* **1999**, *11*, 1, 795.
(8) Yan, H.; Blanford, C. F.; Holland, B. T.; Smyrl, W. H.; Stein, A. *Chem. Mater.* **2000**, *12*, 1134.
(9) Yan, H.; Blanford, C. F.; Holland, B. T.; Parent, M.; Smyrl, W. H.; Stein, A. *Adv. Mater.* **1999**, *11*, 1003.
(10) Imhof, A.; Pine, D. J. *Nature* **1997**, *389*, 948.
(11) Manoharan, V. N.; Imhof, A.; Thorne, J. D.; Pine, D. J. *Adv. Mater.* **2001**, *13*, 447.
(12) Velev, O. D.; Jede, T. A.; Lobo, R. F.; Lenhoff, A. M. *Nature* **1997**, *389*, 447.
(13) Velev, O. D.; Jede, T. A.; Lobo, R. F.; Lenhoff, A. M. *Chem. Mater.* **1998**, *10*, 3597.
(14) Velev, O. D.; Kaler, E. W. *Adv. Mater.* **2000**, *12*, 531.
(15) Wijnhoven, J. E.; Vos, W. L. *Science* **1998**, *281*, 802.
(16) Wijnhoven, J. E.; Zevenhuizen, S.; Hendriks, M.; Vanmaekelbergh, D.; Kelly, J.; Vos, W. L. *Adv. Mater.* **2000**, *12*, 888.
(17) Wang, D.; Caruso, R. A.; Caruso, F. *Chem. Mater.* **2001**, *13*, 364.
(18) Carreon, M. A.; Guliants, V. V. *Chem. Commun.* **2001**, 1438.

10.1021/cm0117376 CCC: $22.00
Published on Web 05/09/2002

Table 1. Synthesis Conditions and Properties of Macroporous[a] and Conventional VPO Phases

sample	VPO source	general description	crystalline phase	surface area (m^2/g)	avg V oxidation state
1[b]	$VO[CHO(CH_3)_2]_3$ H_3PO_3	calcined at 723 K	$VOPO_4 \cdot 2H_2O$	64	4.4
2[b]	$VO[CHO(CH_3)_2]_3$ H_3PO_3	Soxhlet-extracted	$VOPO_4 \cdot 2H_2O$	50	4.0
3[b]	V_2O_5 H_3PO_3	calcined at 723 K	$VOPO_4 \cdot 2H_2O$	41	4.3
4[b]	V_2O_5 H_3PO_3	Soxhlet-extracted	$VOPO_4 \cdot 4H_2O$ β-$VOHPO_4 \cdot 2H_2O$	75	4.1
5[b]	V_2O_5 H_3PO_4	calcined at 723 K	$(VO)_2P_2O_7$	44	4.3
6[c]	V_2O_5 H_3PO_4	aqueous VPO calcined at 673 K	$(VO)_2P_2O_7$	7	4.3
7[c]	V_2O_5 H_3PO_4	organic VPO calcined at 673 K	$(VO)_2P_2O_7$	17	4.3
8[c]	V_2O_5 H_3PO_3	phosphite VPO calcined at 673 K	$(VO)_2P_2O_7$	10	4.5

[a] For macro-VPO phases: Alcohol/vanadium precursor ratio (wt/wt) was 1, 3, 5, 10, and 10 for samples 1−5, respectively. Vanadium precursor/PS sphere ratio (wt/wt) was 2, 2, 6, 6, and 5 for samples 1−5, respectively. Ethanol was used as a solvent for samples 1−4 and isobutanol for sample 5. [b] Macroporous. [c] Conventional.

details of the synthesis and characterization of macro-VPO phases that demonstrate the promise of this novel approach for the molecular engineering of bulk mixed metal oxides for the selective oxidation of lower alkanes.

Experimental Section

Materials. V_2O_5 (Aldrich), $VO[CHO(CH_3)_2]_3$ (99%, Alfa Aesar), H_3PO_3, and H_3PO_4 (85%, Fisher Chemicals) were used as the vanadium and phosphorus sources, respectively. Ethanol and isobutanol (Aldrich) were used as solvents. $NH_2OH \cdot HCl$ (Fisher Scientific) was used as the reducing agent. Monodisperse polystyrene spheres (~400 nm in diameter) were synthesized by an emulsion polymerization process described elsewhere.[7] The ordered close-packed colloidal arrays of spheres were obtained by sedimentation or centrifugation of polystyrene sphere suspensions.

Synthesis of Macroporous VPO Phases. In a typical synthesis, close-packed arrays of polystyrene spheres were deposited on filter paper in a Buchner funnel under vacuum and impregnated with phosphoric or phosphorous acid solutions in anhydrous ethanol. Then, a solution of the vanadium source in anhydrous ethanol was added dropwise to the polystyrene spheres under suction, and the resulting composite was dried in air overnight. The polystyrene spheres were removed from the as-synthesized macroporous VPO by either calcination in air at 723 K for 2−12 h (heating rate = 5 °C/min) or Soxhlet extraction using a mixture of acetone and tetrahydrofuran (1:1 volume ratio). Typical synthesis compositions were (on a weight basis) ethanol/vanadium precursor = 1−10, vanadium precursor/spheres = 2−6. In all experiments, the P/V molar ratio was kept constant at 1.1, which provides the optimal bulk VPO composition for the partial oxidation of *n*-butane.

A different synthesis procedure for macro-VPO phases was employed when V_2O_5 was used as the vanadium source. V_2O_5 was refluxed in isobutanol or ethanol for 16 h. H_3PO_3 or H_3PO_4 dissolved in the same alcohol and polystyrene spheres were added to this vanadium-containing blue/green slurry, followed by another 20 h of refluxing (Figure 1). The resultant blue slurry was filtered, washed with a small quantity of isobutanol, and dried in air at 393 K. The synthesis conditions are shown in Table 1.

Synthesis of Conventional VPO Phases. For comparison, three VPO phases were synthesized using conventional synthesis methods. In all of the syntheses, the P/V molar ratio was 1.1.

Aqueous VPO Precursor. The so-called "aqueous" VPO precursor ($VOHPO_4 \cdot 0.5H_2O$) was prepared according to the synthesis procedure reported by Yamazoe et al.[19] A solution of $NH_2OH \cdot HCl$ (5 g) and H_3PO_4 (85 wt %, 13.94 g) in 150 mL of deionized water was heated under stirring to 353 K. V_2O_5 (10 g) was slowly added to this solution, and a color change from orange to blue/green due to reduction of V^{5+} was noted. The solvent was evaporated in air, and the blue/green solid was dried at 393 K. The soluble $VO(H_2PO_4)_2$ impurity was removed from the $VOHPO_4 \cdot 0.5H_2O$ precursor by boiling in water.

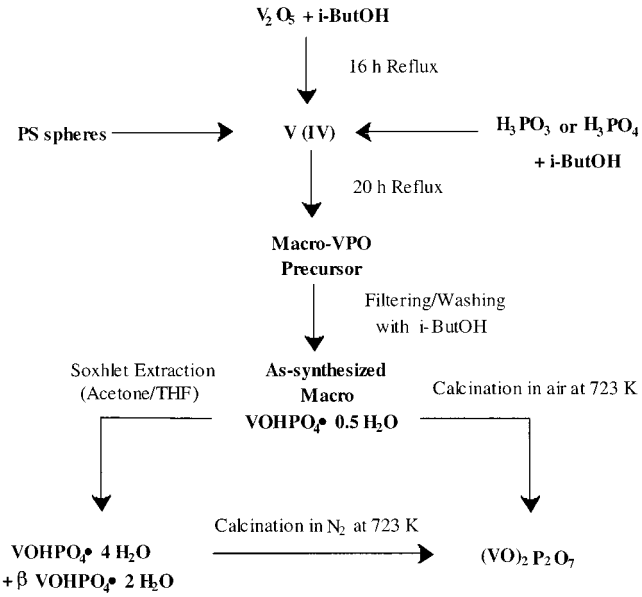

Figure 1. Synthesis of macroporous VPO phases.

Organic VPO Precursor. The organic $VOHPO_4 \cdot 0.5H_2O$ precursor was prepared according to a modified published procedure.[20] V_2O_5 (20 g) was reduced by refluxing in isobutanol (220 mL) for 14 h. Anhydrous orthophosphoric acid (H_3PO_4, 27.88 g) dissolved in isobutanol (20 mL) was added slowly over a period of 2 h to this blue/green suspension, which was refluxed for another 20 h. The resultant blue slurry ($VOHPO_4 \cdot 0.5H_2O$) was filtered, washed with small quantities of isobutanol and acetone, and dried in air at 393 K.

Phosphite VPO Precursor. The phosphite precursor, $VOHPO_3 \cdot 1.5H_2O$, was synthesized according to a procedure described elsewhere.[21] V_2O_5 (10 g, 55 mmol) was refluxed in absolute ethanol (200 mL) for 16 h. A color change from orange to green

(19) Morishige, H.; Tamaki, J.; Miura, N.; Yamazoe, N. *Chem. Lett.* **1990**, 1513.
(20) Bergna, H. E. U.S. Patent 4,769,477, 1988.
(21) Guliants, V. V.; Benziger, J. B.; Sundaresan, S. *Chem. Mater.* **1995**, *7*, 1485.

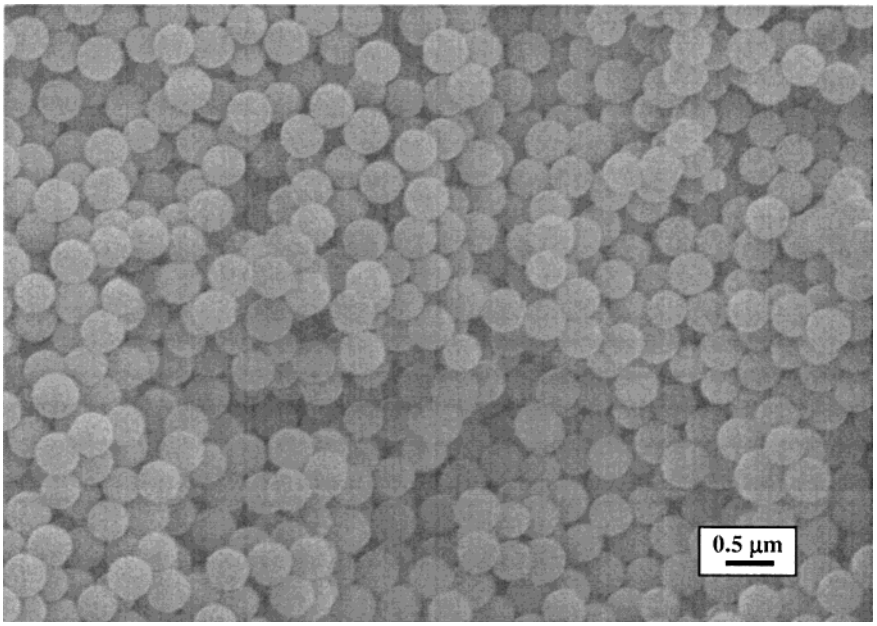

Figure 2. SEM image of sedimented colloidal arrays of ~400-nm polystyrene spheres used as a template in the macro-VPO synthesis.

indicated reduction of V^{5+}. The slurry was cooled to room temperature, and H_3PO_3 (10 g) dissolved in absolute ethanol (80 mL) was added. The mixture was refluxed for another 20 h, and the blue slurry obtained was cooled, filtered, and washed with absolute ethanol. The solid was dried at 393 K for 16 h.

The conventional VPO precursors were activated at 673 K for 8 days in a 1.2% butane/air mixture to obtain the "equilibrated" catalytic $(VO)_2P_2O_7$ phase.

Characterization. Powder XRD patterns were recorded on a Siemens D-500 diffractometer using Cu Kα radiation with step size of 0.02°/s. N_2 BET specific surface areas were determined using a Micromeritics Gemini 2360 analyzer. Scanning electron micrographs were recorded on a Hitachi S-3200N SEM. HRTEM was performed with a JEOL 2010F transmission electron microscope. Chemical analyses were carried out for P and V at Galbraith Laboratories, Inc., Knoxville, TN. Infrared spectra were collected on a Bio-Rad FTS-60 IR spectrometer. The average oxidation state of vanadium was determined by a double titration method.[22]

Results and Discussion

The formation of macroporous VPO phases involves three major steps: (1) deposition of the appropriate vanadium and phosphorus precursor species at the surface of polystyrene spheres via hydrogen bonding, followed by (2) condensation of the inorganic framework around the spheres upon drying, and finally, (3) template removal from the inorganic−organic composite by either calcination or Soxhlet extraction.

Macro-VPO phases were obtained using both sedimented and centrifuged polystyrene sphere templates. Figure 2 shows the monodisperse arrays of sedimented polystyrene spheres. This type of PS array was relatively disordered and led to "termite nest" VPO architectures. A typical SEM image of these macro-VPO phases after template removal by calcination is shown in Figure 3. This macroporous structure displayed interconnected ~200-nm pores inside spherical ~400-nm cavities left after PS sphere removal. The wall thickness estimated from SEM was ~90 nm. The average crystal size determined by the Scherrer method[23] was ~20 nm, indicating that the wall was only 4−5 crystals thick. It is very important to mention that the walls of this macro-VPO structure were composed of nanocrystals, the proposed active and selective phase for the partial oxidation of *n*-butane to maleic anhydride.

In the second approach, PS spheres were packed into ordered arrays by centrifugation. Figure 4 shows ordered hexagonal close-packed arrays of spheres obtained by centrifugation of polystyrene suspensions at ~1000 rpm. Highly ordered VPO phases obtained by infiltration and condensation of the VPO precursor species inside these hexagonal sphere arrays, followed by template removal, are shown in Figure 5. The observed "honeycomb" macro-VPO architecture showed interconnected ~100-nm pores inside spherical ~300-nm cavities. The wall thickness for this highly ordered macrostructure was ~50 nm. The walls of this macro-VPO structure were composed of the $VOPO_4 \cdot 2H_2O$ phase.

The typical synthesis conditions, specific surface areas, crystalline phases, and the average vanadium oxidation states for conventional and macro-VPO phases are shown in Table 1. VPO phases obtained by conventional methods exhibited only low surface areas, 7−17 m^2/g. On the other hand, the macro-VPO phases showed much higher surface areas, ~44−75 m^2/g, after the removal of polystyrene spheres. It is important to mention that the surface areas of the macro-VPO phases were consistent with an XRD-based estimate for the 20-nm crystals of $(VO)_2P_2O_7$ comprising the walls of the macro-VPO phases. The high surface areas observed indicated that most of the macropores in both ordered and disordered macro-VPO phases were interconnected. When $VO[CHO(CH_3)_2]_3$ was used as a source during synthesis, the yield of macro-VPO phases after sphere

(22) Hodnett, B. K.; Permanne, P.; Delmon, B. *Appl. Catal.* **1983**, *6*, 231.

(23) Cullity, B. D.; Stock, S. R. *Elements of X-ray Diffraction*; Prentice Hall: Upper Saddle River, NJ, 2001.

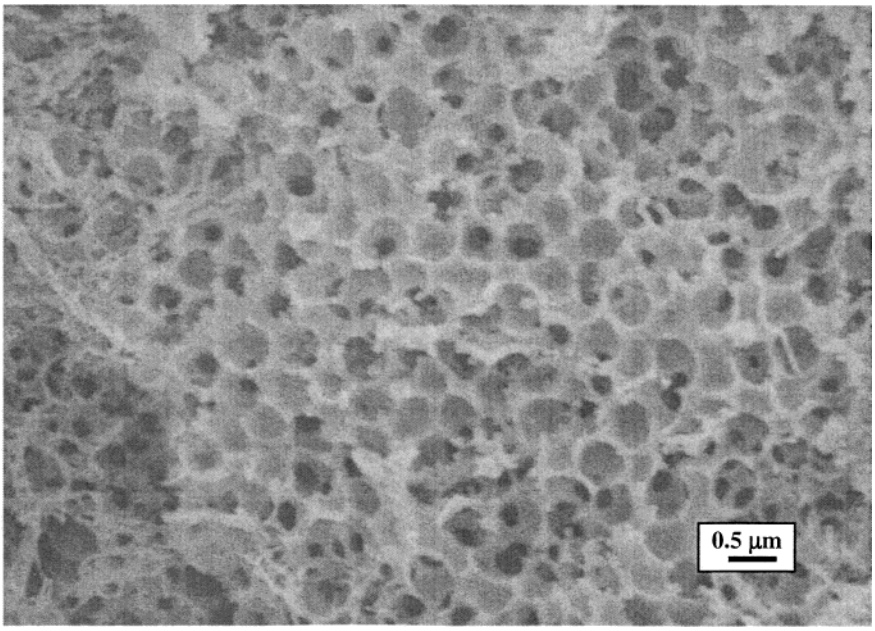

Figure 3. SEM image of macro-VPO prepared using sedimented spheres and calcined in air at 723 K (sample 5 in Table 1).

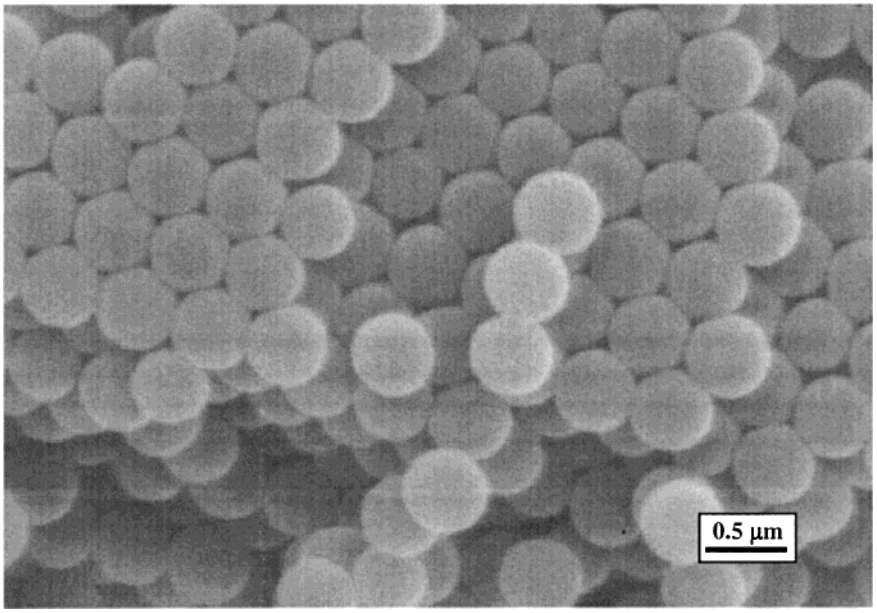

Figure 4. SEM image of centrifuged colloidal crystal arrays of ~400-nm polystyrene spheres used as a template in the macro-VPO synthesis.

removal by calcination in air or Soxhlet extraction was in the ~15% range of the original composite material, the rest being dense nonmacroporous VPO phases. The yield of macro-VPO was very high (~80%) when V_2O_5 was used in the synthesis (Figure 1).

The findings presented in Table 1 indicate that it is possible to obtain different crystalline VPO phases by appropriately choosing the VPO sources and a template removal method (calcination or Soxhlet extraction). It is generally agreed that vanadyl pyrophosphate, $(VO)_2P_2O_7$, is the catalytically active and selective phase in the oxidation of *n*-butane to maleic anhydride over the VPO catalysts.[1,4,24,25] Table 1 shows that macro-VPO sample 5 contained $(VO)_2P_2O_7$ as the only crystalline phase. However, all other VPO phases ($VOPO_4 \cdot 2H_2O$, $VOHPO_4 \cdot 2H_2O$, and β-$VOHPO_4 \cdot 2H_2O$) present in the macroporous samples 1−4 are immediate precursors for $(VO)_2P_2O_7$. For instance, $VOPO_4 \cdot 2H_2O$ can be transformed to $(VO)_2P_2O_7$ by reduction in alcohol and subsequent thermal treatment in N_2.[25] $VOHPO_4 \cdot 2H_2O$ and β-$VOHPO_4 \cdot 2H_2O$ can be directly transformed to $(VO)_2P_2O_7$ by dehydration at 773 K in N_2.[25] These phase transformations occurred with only a slight decrease in the structural order. However, the high surface areas observed for the different crystalline macro-VPO phases were not affected by these phase transformations. The average oxidation state of vanadium for Soxhlet-extracted samples was 4.0−4.1. For calcined samples, the average oxidation state was somewhat higher (4.3−4.5), probably because of the oxidizing activation conditions (723 K in air). It is generally believed that an

(24) Cavani, F.; Trifiro, F. *Appl. Catal. A: Gen.* **1992**, *85*, 115.
(25) Guliants, V. V.; Benziger, J. B.; Sundaresan, S.; Wachs, I. E.; Jehng, J. M.; Roberts, J. E. *Catal. Today* **1996**, 28, 275.

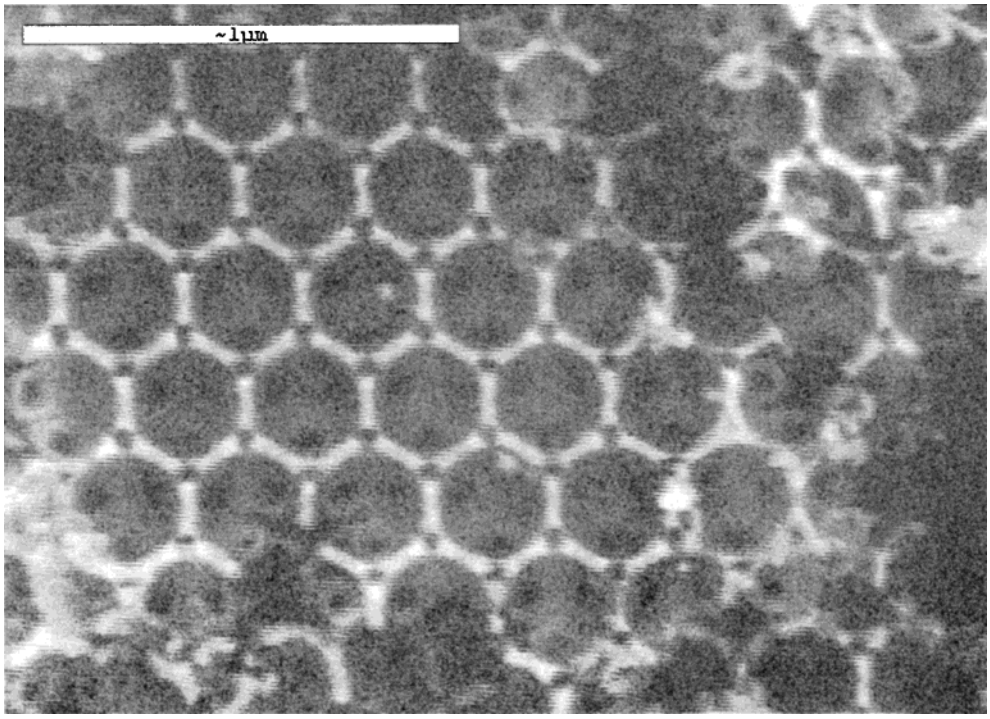

Figure 5. SEM image of macro-VPO prepared using centrifuged spheres and calcined in air at 723 K (sample 1 in Table 1).

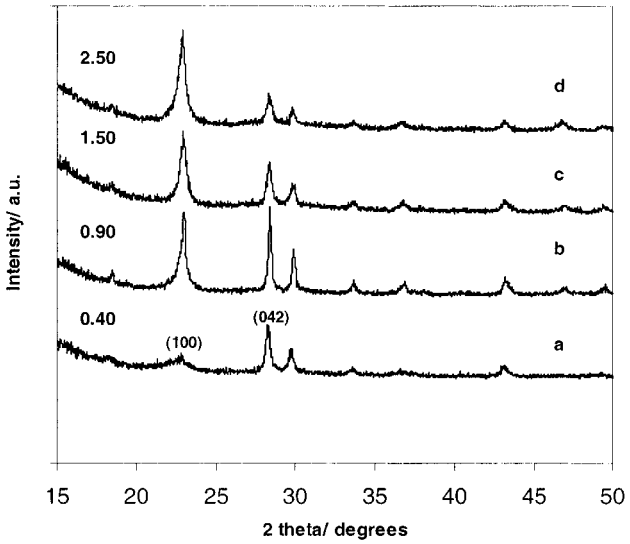

Figure 6. XRD patterns of conventional (a) phosphite, (b) aqueous, (c) organic, and (d) macro-VPO phases (sample 5 in Table 1). Numbers on the left-hand side indicate the intensity ratios (I_{100}/I_{042}) of the interplanar (100) and in-plane (042) XRD reflections of $(VO)_2P_2O_7$.

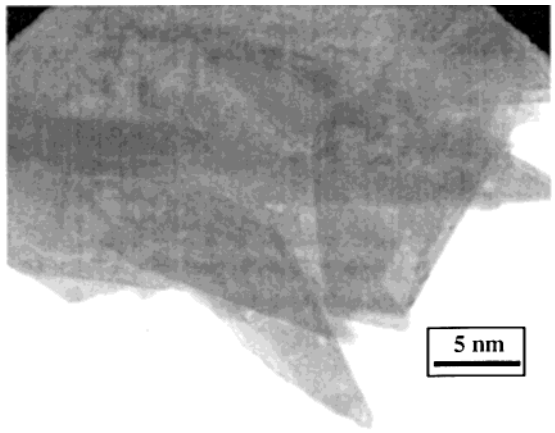

Figure 7. TEM image showing the walls of the macroporous $(VO)_2P_2O_7$ phase composed of ~20-nm crystallites (sample 5 in Table 1).

average vanadium oxidation state in the 4.1−4.3 range is optimal for the selective oxidation of *n*-butane.[4,22,24] Therefore, these macro-VPO phases are promising for the partial oxidation of *n*-butane. Furthermore, the ICP elemental analysis revealed that the novel macro-VPO phases also display optimal bulk compositions (P/V ≈ 1.05) for superior catalytic performance in the oxidation of *n*-butane to maleic anhydride. The slight excess of phosphorus stabilized V^{4+} relative to the V^{5+} oxidation state, leading to the observed average vanadium oxidation states in the macro-VPO samples.

Further insights into the microstructure of these macro-VPO phases were obtained from the XRD and HRTEM studies. The XRD patterns for macro-VPO (sample 5) and conventional VPO phases (samples 6−8) are shown in Figure 6. Among the macro-VPO phases, sample 5 was studied in particular detail because it contained the proposed active and selective $(VO)_2P_2O_7$ phase. The XRD patterns of the macro-VPO and conventional VPO phases show the presence of $(VO)_2P_2O_7$ as the only crystalline phase. The (100) surface planes of $(VO)_2P_2O_7$ have been proposed to contain the active and selective surface sites for *n*-butane oxidation to maleic anhydride. Previously, the intensity ratio of the interplanar (100) and in-plane (042) XRD reflections of vanadyl pyrophosphate (I_{100}/I_{042}) has been employed as an indicator of the preferential exposure and the stacking order of the (100) planes.[25] The conventional VPO phases exhibited low intensity ratios (0.4, 0.9, and 1.5 for the phosphite, aqueous, and organic VPO phases, respectively), indicating that the (100) planes were not dominant in these phases. On the other hand, the macroscale-templated synthesis yielded much higher

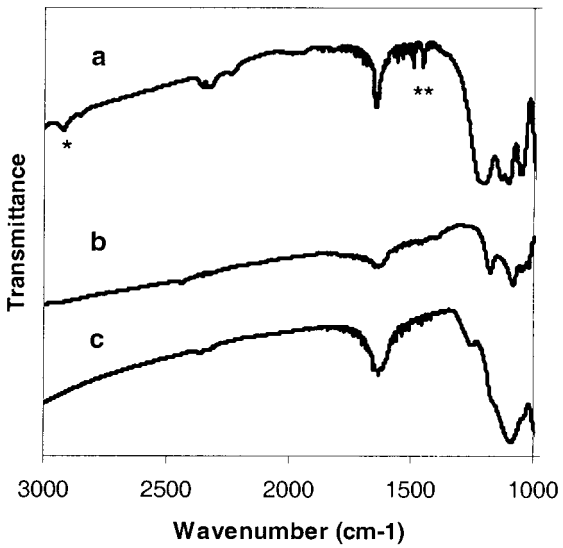

Figure 8. Infrared spectra of (a) as-synthesized, (b) Soxhlet-extracted, and (c) calcined macroporous $(VO)_2P_2O_7$ (sample 5 in Table 1). The stars denote C−H stretching vibration modes of polystyrene.

intensity ratios, $I_{100}/I_{042}=2.5$, suggesting that macroporous VPO phases exposed the (100) planes of vanadyl pyrophosphate to much greater degree than the conventional VPO catalysts. The higher exposure of the (100) plane of $(VO)_2P_2O_7$ in macro-VPO as compared to conventional VPO can be explained by a unique confined environment for the nucleation and growth of the hemihydrate precursor, $VOHPO_4{\cdot}0.5H_2O$. The dimensions of the interstitial voids in the PS sphere arrays restricted the growth of the VPO precursor crystals heterogeneously nucleated at the surface of PS spheres. This led to the formation of many small crystallites (Figure 7), with preferential exposure of the (100) planes of $(VO)_2P_2O_7$ after precursor transformation. Figure 7 shows the characteristic platelet morphology of the $(VO)_2P_2O_7$ crystals. These ∼20 nm crystals form the walls of the macro-VPO structure.

Figure 8 shows the IR spectra of the as-synthesized, Soxhlet-extracted, and calcined macro-VPO phases (sample 5). The as-synthesized macro-VPO showed the characteristic bands of vanadyl(IV) phosphite.[21] The stretching bands of V−O−V and V═O appear at 683−642 and 1044−972 cm^{-1}, respectively.[26] The stretching vibrations for P−O−P, P═O, PO_3, P−OH, and P−H are present at 930, 1198, 1126−1090, 3371, and 2350−2250 cm^{-1}, respectively.[27] The sharp peak at 1640 cm^{-1} was associated with surface-adsorbed water. The two bands at 1440 and 1495 cm^{-1} correspond to the symmetric and asymmetric C−H deformation vibrations of polystyrene, respectively. Also, C−H stretching vibrations are present at ∼2920−2850 cm^{-1}. The Soxhlet-extracted and calcined macro-VPO phases show similar vibrational modes for the vanadium and phosphate species. However, the vibrational modes of the organic template at 1440, 1495, and 2920−2850 cm^{-1} were absent, indicating that the polystyrene spheres were completely removed.

Conclusions

The macroscale-templated route offers a novel and unique approach for the rational design of bulk mixed metal oxides with desirable structural, compositional, and morphological properties that are critical for superior catalytic performance in the partial oxidation of lower alkanes. We described here the first successful example of such hierarchically structured bulk mixed metal oxide phases (macro-VPO) displaying unprecedented high surface areas (75 m^2/g); desirable pore architectures; optimal chemical environments (bulk compositions and vanadium oxidation states); and preferential exposure of the (100) surface plane of $(VO)_2P_2O_7$, the proposed active and selective phase for *n*-butane oxidation. We anticipate that this method will also be highly promising for the molecular engineering of other catalytic mixed metal oxides.

Acknowledgment. The authors acknowledge Dr. Nan Yao (Princeton Materials Institute) for the TEM image of the macro-VPO.

CM0117376

(26) Socrates, G. *Infrared Characteristic Group Frequencies*; Wiley: New York, 1994.
(27) Abe, T.; Taguchi, A.; Iwamoto, M. *Chem. Mater.* **1995**, *7*, 1429.